[1]

Contact: francesca.bellini@cern.ch

Testing production scenarios for (anti-)(hyper-)nuclei with multiplicity-dependent measurements at the LHC

F. Bellini (CERN, Geneva)
and A. P. Kalweit (CERN, Geneva)

The production of light anti- and hyper-nuclei provides unique observables to characterise the system created in high energy proton-proton (pp), proton-nucleus (pA) and nucleus-nucleus (AA) collisions. In particular, nuclei and hyper-nuclei are special objects with respect to non-composite hadrons (such as pions, kaons, protons, etc.), because their size is comparable to a fraction or the whole system created in the collision. Their formation is typically described within the framework of coalescence and thermal-statistical production models. In order to distinguish between the two production scenarios, we propose to measure the coalescence parameter B_A for different anti- and hyper-nuclei (that differ by mass, size and internal wave-function) as a function of the size of the particle emitting source. The latter can be controlled by performing systematic measurements of light anti- hyper- nuclei in different collision systems (pp, pA, AA) and as a function of the multiplicity of particles created in the collision. While it is often argued that the coalescence and the thermal model approach give very similar predictions for the production of light nuclei in heavy-ion collisions, our study shows that large differences can be expected for hypernuclei with extended wave-functions, as the hyper-triton. We compare the model predictions with data from the ALICE experiment and we discuss perspectives for future measurements with the upgraded detectors during the High-Luminosity LHC phase in the next decade.

1. Introduction

In the last few years A Large Ion Collider Experiment (ALICE) Collaboration has reported on the measurement of the production of light nuclei in pp, p–Pb and Pb–Pb collisions at TeV centre-of-mass energies [], based on data collected during the first ten years of operations of the CERN Large Hadron Collider (LHC). The measurements of deuteron, ,

* Proceedings of the XXV Cracow EPIPHANY Conference on Advances in Heavy Ion Physics

Mass number	Nucleus	Composition	B_E (MeV)	Spin J_A	(Charge) rms radius ${\lambda_A}^{meas}$ (fm)	Harmonic oscillator size parameter r_A (fm)	Refs.
A = 2	d	pn	2.224575 (9)	1	2.1413 ± 0.0025	3.2	[1,2]
A = 3	^{3}H	pnn	8.4817986 (20)	1/2	1.755 ± 0.086	2.15	[3]
	^{3}He	ppn	7.7180428 (23)	1/2	1.959 ± 0.030	2.48	[3]
	$^{3}_{\Lambda}$H	pΛn	0.13 ± 0.05	1/2	4.9 – 10.0	6.8 – 14.1	[4,5]
A = 4	^{4}He	ppnn	28.29566 (20)	0	1.6755 ± 0.0028	1.9	[6,7]
	$^{4}_{\Lambda}$H	pΛnn	2.04 ±0.04	0	2.0 – 3.8	2.4 – 4.9	[4,5]
	$^{4}_{\Lambda\Lambda}$H	pΛΛn	0.39 – 0.51	1	4.2 – 7.1	5.5 – 9.4	[5]
	$^{4}_{\Lambda}$He	ppΛn	2.39 ± 0.03	0	2.0 – 3.8	2.4 – 4.9	[4,5]

Table 1. Properties of nuclei and hyper-nuclei with mass number $A \leq 4$. B_E is the binding energy in MeV. The size of the nucleus is given in terms of the (charge) rms radius of the wave-function, λ_A. The size parameter of the wave-function of the harmonic oscillator potential, r_A, is chosen such that the measured/expected rms is approximately reproduced. Please note that the proton rms charge radius $\lambda_p = 0.879(8)$ fm [8] is subtracted quadratically from the measured rms charge radius λ_A^{meas} of the nucleus $\lambda_A = \sqrt{(\lambda_A^{meas})^2 - \lambda_p^2}$ to account for the finite extension of the constituents. Implicitly we assume here that $\lambda_\Lambda \approx \lambda_n \approx \lambda_p$. References are given in the last column. The spin of $^{4}_{\Lambda\Lambda}$H is discussed in the text of [5].

2. The coalescence approach

Starting from the model described in [9, 10], we have obtained in [11] a generalised expression for the coalescence parameter B_A

$$\boxed{B_A = \frac{2J_A+1}{2^A}\frac{1}{\sqrt{A}}\frac{1}{m_T^{A-1}}\Big(\frac{2\pi}{R^2+(\frac{r_A}{2})^2}\Big)^{\frac{3}{2}(A-1)}} \quad , \tag{1}$$

which is a function of the spin of the particle J_A, its transverse mass $m_{\rm T}$, its size parameter r_A and the source radius R. Figure 2 shows the source radius dependence of B_A for different composite objects, including the nuclei and hyper-nuclei with $A = 2, 3$ and 4 whose properties are reported in Tab. 1.

2.1. Comparison with data

REFERENCES

[1] C. Van Der Leun and C. Alderliesten, "The deuteron binding energy," *Nucl. Phys.* **A380** (1982) 261–269.

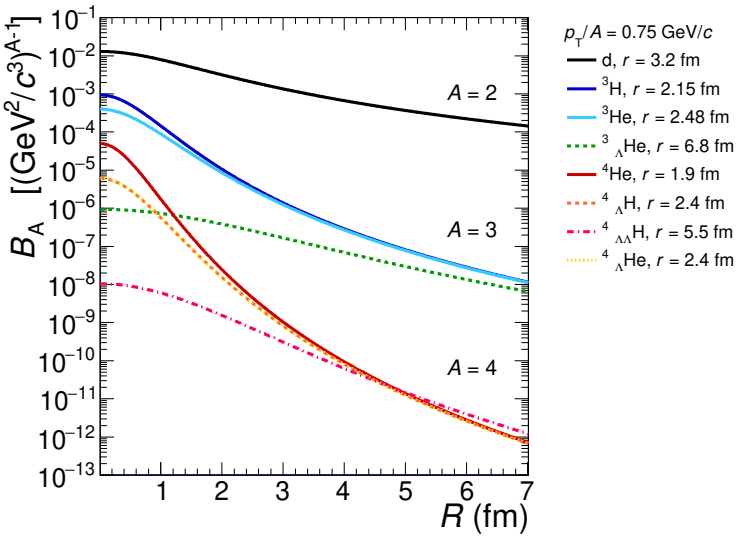

Fig. 1. (Color online) Coalescence parameter B_A as a function of the source radius R as predicted from the coalescence model (Eq. 1) for various composite objects with p_T/A = 0.75 GeV/c. For each (hyper-)nucleus, the radius r used for the calculation is reported in the legend.

[2] P. J. Mohr, D. B. Newell, and B. N. Taylor, "CODATA Recommended Values of the Fundamental Physical Constants: 2014," *Rev. Mod. Phys.* **88** no. 3, (2016) 035009, arXiv:1507.07956 [physics.atom-ph].

[3] J. E. Purcell and C. G. Sheu, "Nuclear Data Sheets for A = 3," *Nucl. Data Sheets* **130** (2015) 1–20.

[4] D. H. Davis, "50 years of hypernuclear physics. I. The early experiments," *Nucl. Phys.* **A754** (2005) 3–13.

[5] H. Nemura, Y. Suzuki, Y. Fujiwara, and C. Nakamoto, "Study of light Lambda and Lambda-Lambda hypernuclei with the stochastic variational method and effective Lambda N potentials," *Prog. Theor. Phys.* **103** (2000) 929–958, arXiv:nucl-th/9912065 [nucl-th].

[6] M. Wang, G. Audi, F. Kondev, W. Huang, S. Naimi, and X. Xu, "The AME2016 atomic mass evaluation (II). Tables, graphs and references," *Chinese Physics C* **41** no. 3, (2017) 030003.

[7] I. Angeli and K. P. Marinova, "Table of experimental nuclear ground state charge radii: An update," *Atom. Data Nucl. Data Tabl.* **99** no. 1, (2013) 69–95.

[8] **A1** Collaboration, J. C. Bernauer *et al.*, "High-precision determination of the electric and magnetic form factors of the proton," *Phys. Rev. Lett.* **105** (Dec, 2010) 242001.

[9] R. Scheibl and U. W. Heinz, "Coalescence and flow in ultrarelativistic heavy ion collisions," *Phys. Rev.* **C59** (1999) 1585–1602, arXiv:nucl-th/9809092 [nucl-th].

[10] K. Blum, K. C. Y. Ng, R. Sato, and M. Takimoto, "Cosmic rays, antihelium, and an old navy spotlight," *Phys. Rev.* **D96** no. 10, (2017) 103021, arXiv:1704.05431 [astro-ph.HE].

[11] F. Bellini and A. P. Kalweit, "Testing coalescence and statistical-thermal production scenarios for (anti-)(hyper-)nuclei and exotic QCD objects at LHC energies," arXiv:1807.05894 [hep-ph].

[12] **ALICE** Collaboration, S. Acharya *et al.*, "Production of deuterons, tritons, ^{3}He nuclei and their anti-nuclei in pp collisions at $\sqrt{s} = 0.9$, 2.76 and 7 TeV," *Phys. Rev.* **C97** no. 2, (2018) 024615, arXiv:1709.08522 [nucl-ex].

[13] **ALICE** Collaboration, J. Adam *et al.*, "Production of light nuclei and anti-nuclei in pp and Pb-Pb collisions at energies available at the CERN Large Hadron Collider," *Phys. Rev.* **C93** no. 2, (2016) 024917, arXiv:1506.08951 [nucl-ex].

[14] **ALICE** Collaboration, J. Adam *et al.*, "$^3_\Lambda$H and $^{\overline{3}}_{\overline{\Lambda}}\overline{\mathrm{H}}$ production in Pb-Pb collisions at $\sqrt{s_{\mathrm{NN}}} = 2.76$ TeV," *Phys. Lett.* **B754** (2016) 360–372, arXiv:1506.08453 [nucl-ex].

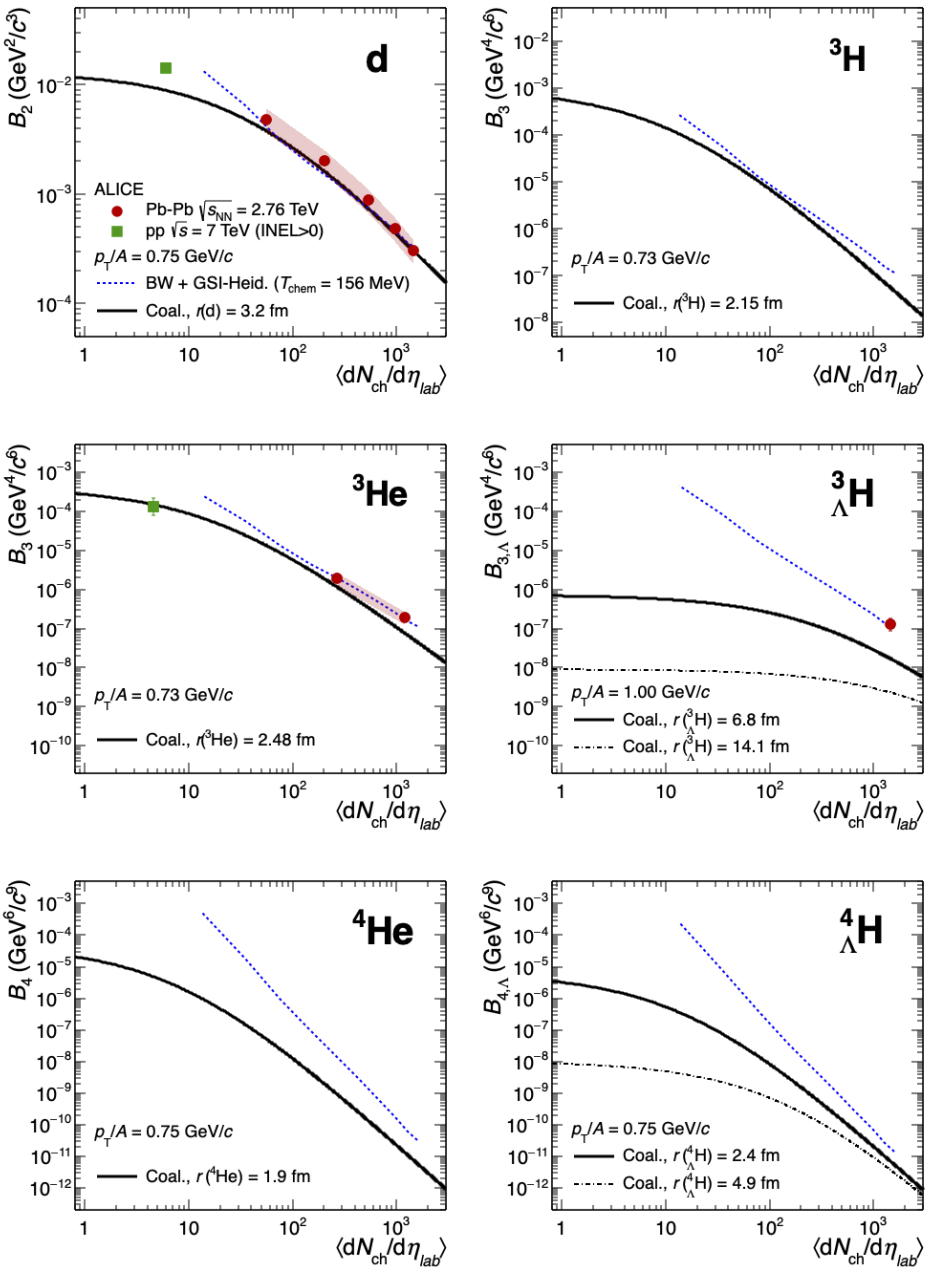

Fig. 2. (Color online) Coalescence parameter B_A as a function of the average charged particle multiplicity density for various (hyper-)nuclei, up to $A = 4$. The coalescence calculations (continuous or dashed-dotted black lines) are compared to the thermal+blast-wave predictions (dashed blue line), as well as to pp (green square) and Pb–Pb (red circles) collision data from ALICE [12–14].